

# Towards Calibrated Deep Clustering Network

Yuheng Jia<sup>1</sup>, Jianhong Cheng<sup>1</sup>, Hui Liu<sup>2</sup>, Junhui Hou<sup>3</sup>

<sup>1</sup> School of Computer Science and Engineering, Southeast University, Nanjing 210096, China

<sup>2</sup> School of Computing and Information Sciences, Caritas Institute of Higher Education, Hong Kong

<sup>3</sup> Department of Computer Science, City University of Hong Kong, Kowloon, Hong Kong

<sup>1</sup>{yhjia, chengjh}@seu.edu.cn, <sup>2</sup>hliu99-c@my.cityu.edu.hk, <sup>3</sup>jh.hou@cityu.edu.hk

## Abstract

Deep clustering has exhibited remarkable performance; however, the overconfidence problem, i.e., the estimated confidence for a sample belonging to a particular cluster greatly exceeds its actual prediction accuracy, has been overlooked in prior research. To tackle this critical issue, we pioneer the development of a calibrated deep clustering framework. Specifically, we propose a novel dual-head deep clustering pipeline that can effectively calibrate the estimated confidence and the actual accuracy. The calibration head adjusts the overconfident predictions of the clustering head using regularization methods, generating prediction confidence and pseudo-labels that match the model learning status. This calibration process also guides the clustering head in dynamically selecting reliable high-confidence samples for training. Additionally, we introduce an effective network initialization strategy that enhances both training speed and network robustness. Extensive experiments demonstrate the proposed calibrated deep clustering framework not only surpasses state-of-the-art deep clustering methods by approximately 10 times in terms of expected calibration error but also significantly outperforms them in terms of clustering accuracy.

## 1. Introduction

Clustering aims to categorize the input samples into distinct groups, where samples within the same group exhibit greater similarity compared to those in other groups, without utilizing any ground-truth supervisory information. Recently, deep learning-based clustering methods, a.k.a. deep clustering, have showcased remarkable clustering performance owing to the powerful feature representation capability of deep neural networks (DNN) [22, 32]. Representative methods such as DEC [38] and ProPos [14] have demonstrated that applying a simple K-means algorithm to features extracted from a DNN can yield commendable clustering performance.

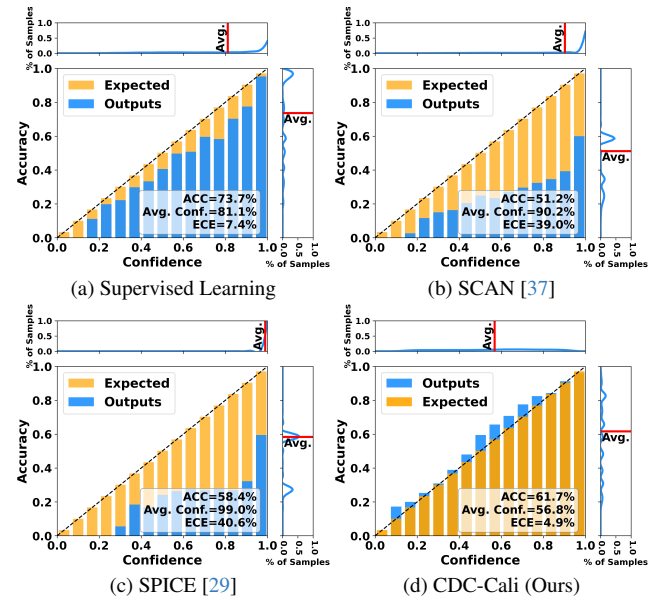


Figure 1. Reliability diagrams of different methods on CIFAR-20. In the ideal case, the confidence of a model’s output should be roughly equal to its accuracy, which means the confidence of the output is well-calibrated. However, the previous deep clustering models faced a severe overconfidence problem, i.e., the estimated confidence largely exceeds its real accuracy. We propose a calibrated deep clustering (CDC) model that gets better-calibrated confidence and better clustering performance.

Training a deep clustering network is generally a very challenging task as no supervisory information is available. Existing methods solve the training dilemma by introducing some side tasks in training the deep clustering network. For example, DEC [38] introduces the auto-encoder (AE) in training the network, and SCAN [37] adopts contrastive learning. Recently, pseudo-labeling that uses the model’s own output as pseudo labels to guide the unsupervised clustering network training through a vanilla loss cross-entropy has become mainstream in deep clustering [29, 32, 37]. Although those methods have achieved remarkable clustering performance, they generally use a *fixed threshold* to select

the pseudo labels, which ignores the learning status of the model, i.e., in the early training stages, a higher threshold will select fewer and class-imbalanced training samples, which depress the convergence speed, while in the later training stages, the fixed threshold is more likely to introduce noisy pseudo-labels due to the increasing confidence in the predictions. More critically, the pseudo-label-based methods will result in a serious overconfidence problem, i.e., the predicted confidence of the model’s output will largely exceed the actual prediction accuracy. As shown in Fig. 1, the overconfidence problem of the state-of-the-art (SOTA) deep clustering methods like SPICE [29] and SCAN [37] is even worse than the supervised learning model, as they rely on the pseudo-labels to train the network, and the inevitable noise in the pseudo-labels aggravates the overconfidence problem. Accurate confidence estimation is important to a machine learning model, especially in building trustworthy decision-making systems like medical diagnosis [24], autonomous vehicles [8], and financial trading [39], which suggests when we can trust the prediction of a learning model. However, confidence calibration has not been studied under deep clustering networks, and the common calibration methods like Temperature Scaling [7, 11, 19] rely on a labeled validation set, which is not applicable in deep clustering. Moreover, some regularization methods like Label Smoothing [26] and Focal Loss [25] can slightly reduce the overconfidence phenomenon, but will significantly depress the clustering performance of the modern deep clustering networks.

**Our Contributions.** *For the first time*, we investigate the construction of a well-calibrated deep clustering network in this paper. Specifically, we propose a dual-head network structure comprising a clustering head and a calibration head. Within the calibration head, we propose a novel calibration approach that penalizes the confidence of predictions generated by the clustering head for all samples. This enables the output of the calibration head to accurately estimate the actual confidence level of the predictions. Meanwhile, within the clustering head, we utilize the calibrated confidence provided by the calibration head to assess the learning progress of each class and selectively choose high-confidence samples for effective pseudo-labeling. These two heads mutually reinforce each other by leveraging information from one another. Additionally, we present an effective initialization approach to initialize both the clustering head and the calibration head, thereby ensuring more stable and rapid training.

Extensive experimental evaluation on six benchmark datasets shows that our model not only surpasses state-of-the-art deep clustering methods by approximately 10 times in terms of expected calibration error (ECE) but also significantly outperforms them in terms of clustering accuracy.

The rest of this paper is organized as follows. We first

review the related works regarding deep clustering and confidence calibration in Section 2, then we introduce the proposed model in detail in Section 3. Afterward, we evaluate our model and compare it with the SOTA deep clustering models in Section 4, and finally conclude this paper in Section 5.

## 2. Related Works

**Deep Clustering** Deep clustering methods can be broadly classified into two categories: *Clustering based on representation learning* which first learn a representation of the data and then apply a clustering model like K-means [13, 36] and Spectral Clustering [1, 30] to obtain the final clustering results, *Iterative deep clustering with self-supervision* which aim to learn the data representation and perform clustering simultaneously under the supervision of self-training [12, 38], self-labeling [29, 32, 37] and contrastive information [22, 34]. Recently, self-labeling methods have demonstrated superior performance by selecting high-confidence instances through thresholding soft assignment probabilities and updating the entire network by minimizing the cross-entropy loss of the selected instances. However, they often use a fixed threshold to determine the assignment of pseudo-labels, which does not take into account the learning status of the model. How to determine a suitable threshold is still a challenging task.

**Confidence Calibration.** Capturing the accurate confidence estimation is important to real-world decision-making systems, like self-driving car [8] and disease diagnosis [24], as in those applications, prediction systems not only should be accurate but also should suggest when they are likely to be not correct. Moreover, accurate confidence estimation is also important to the interpretability of modern neural networks. However, modern neural networks usually face the overconfidence problem, i.e., the estimated confidence by a neural network usually exceeds its real prediction accuracy [9]. To solve this problem, many calibration methods were proposed. Roughly speaking, the existing calibration methods can be divided into two categories: *post-calibration* and *calibration during model training*. Post-calibration calibrates the model’s output after the model finishes the training. For example, Guo et al. [11] proposed Temperature Scaling to achieve output calibration, which learns the temperature in the softmax function by minimizing the maximum likelihood of the most confident samples to adjust its predictions. The second kind of method calibrates the model’s output during the training process. They usually use some regularization techniques to penalize prediction confidence [25, 31, 33]. For example, Label Smoothing [26] uses soft labels to avoid overfitting the network’s predictions. Focal Loss [25] is designed to fit hard samples and prevents easy samples from dominat-

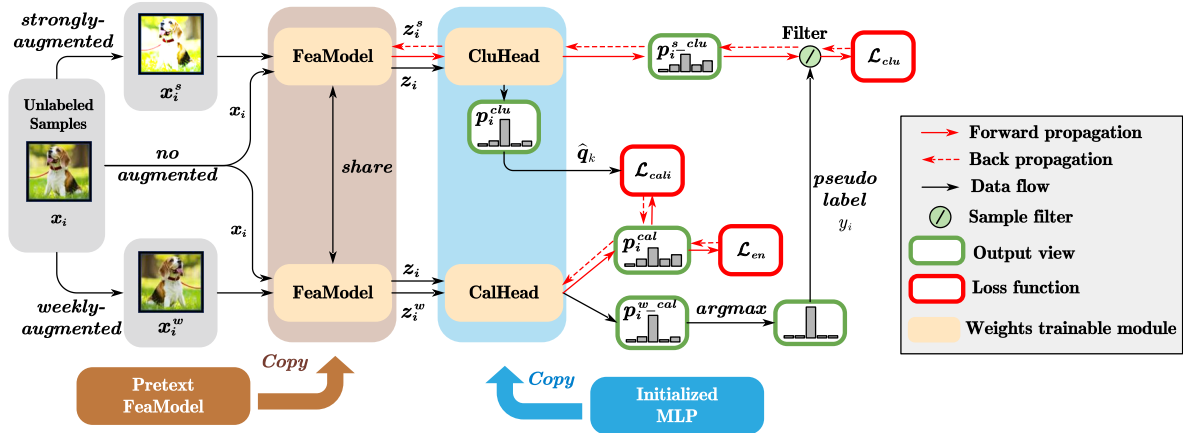


Figure 2. Illustration of the proposed CDC framework. The calibration head uses regularization methods to penalize overconfident predictions from the clustering head. The clustering head, in turn, uses the better confidence provided by the calibration head to generate pseudo-labels and thresholds for each class, and then selects high-confidence samples for training.

ing the training process, implicitly penalizing overconfident predictions. The  $L_p$  Norm [17] directly serves as an additional term to the cross-entropy, limiting the distribution range of logits to control the confidence level.

As demonstrated in Fig. 1, deep clustering faces a more severe overconfidence problem than the supervised learning models. The reason is that the SOTA deep clustering methods rely on pseudo-labeling, which will unavoidably aggravate the overconfidence problem. Unfortunately, this problem has been overlooked in prior research. Moreover, the previous calibration methods can not be directly applied to solve the overconfidence problem in unsupervised clustering, as the post-calibration method needs a labeled validation set to turn its hyper-parameters, while the regularization methods will depress the quality of the selected pseudo labels and accordingly harm the clustering performance. Therefore, in this paper, we study how to build a calibrated deep clustering neural network to achieve both high clustering performance and accurate confidence estimation.

### 3. Proposal Method

As shown in Fig. 2, the proposed model is a dual-head network containing a clustering head and a calibration head. We first pre-train the backbone network by MoCo-v2 [4], and use the proposed initialization strategy to initialize the clustering head and the calibration head. Then, we train the clustering head by selecting high-confidence pseudo-labels through a cross-entropy loss, where the confidence level of samples is estimated by the calibration head. At the same time, we train the calibration head with a novel calibration approach to get an accurate estimation of the confidence of the output of the samples from the clustering head. Finally, the clustering head and the calibration head are optimized

simultaneously to achieve a self-boosting.

#### 3.1. Dual-head Network

Denote by  $\mathcal{D}_u = \{x_i : i \in \{1, 2, \dots, N\}\}$  a training set of  $N$  unlabeled samples. Weak and strong augmentation strategies from [37] are used to obtain  $x_i^w$  and  $x_i^s$  for each sample  $x_i$ . Let  $f(\Theta; x_i)$  be the feature extractor,  $g(\theta; \cdot)$  be the classifier,  $\sigma(\cdot)$  be the softmax function, and  $C$  be the predetermined classes. Then, the output probabilities are  $p_i^w = \sigma(g(\theta; f(\Theta; x_i^w)))$  and  $p_i^s = \sigma(g(\theta; f(\Theta; x_i^s)))$ . In each training batch, we select  $B$  samples from  $\mathcal{D}_u$ . In the remainder of this paper, all the operators are performed in a batch without special mention.

##### 3.1.1 Clustering Head

Similar to the previous deep clustering methods, we use a three-layer Multi-Layer Perceptron (MLP) as the clustering head to generate the clustering result, as shown in Fig. 3.

Due to the lack of ground-truth information, the most crucial issue in training the clustering head is generating highly reliable pseudo labels. Previous methods [29, 32, 37] usually adopt a *fixed* and *predefined* threshold to select samples as the pseudo labels. However, such a fashion overlooks the fact that the model’s output confidence continuously increases during the training process. Specifically, in the early training strategy, the threshold is typically set too high, resulting in the selection of only a limited number of samples and slowing down the training speed. As training progresses, the confidence of all samples increases, leading to the selection of more samples as pseudo labels. Consequently, more incorrect pseudo labels are included, negatively impacting the clustering performance.

Furthermore, as previously analyzed, deep clustering networks face a significant overconfidence problem, where

the model’s confidence in its predictions surpasses its true accuracy. This overconfidence issue hinders the model’s ability to perceive its learning status, further complicating the determination of an appropriate threshold. Additionally, previous methods utilize a single global threshold for all classes, which biases the model towards selecting more samples from easy classes (those with higher confidence) while disregarding hard classes (those with lower confidence).

To address these challenges, we use the confidence estimated by the calibration head (which will be introduced later) to determine the threshold. This approach allows a more accurate estimation of the model’s learning status. Additionally, we adopt different thresholds for different classes, which helps mitigate the discrepancies in data utilization across categories.

Specifically, we first calculate the average confidence of each cluster in the calibration head, i.e.,

$$\mathbf{p}_{avg-c} = \sum_{i \in S_c^{cal}} \frac{\mathbf{p}_i^{w-cal}}{|S_c^{cal}|}, \forall c = 1, 2, \dots, C, \quad (1)$$

where  $\mathbf{p}_i^{w-cal}$  denotes the confidence of the weak augmentation of  $\mathbf{x}_i$  estimated by the calibration head,  $S_c^{cal}$  is the set of samples being categorized to the  $c$ -th cluster by the calibration head,  $|S_c^{cal}|$  indicates the total number of samples belong to the  $c$ -th cluster, and  $\mathbf{p}_{avg-c}$  denotes the average confidence of the samples belonging to the  $c$ -th cluster estimated by the calibration head. The average confidence of each cluster estimated by the calibration head can well capture the learning status of each cluster, i.e., if  $\mathbf{p}_{avg-c}$  is large, the model is more confident about the prediction for the samples in the  $c$ -th cluster; accordingly, we should select more samples from this cluster as the pseudo-labels. We determine the number of samples selected as the pseudo-labels for the  $c$ -th cluster via

$$M_c = \mathbf{p}_{avg-c} \times \lfloor B/C \rfloor, \quad (2)$$

where  $\lfloor \cdot \rfloor$  denotes the lower approximation operator. Finally, we select the top  $M_c$  samples from each cluster to constitute the final pseudo-labeled samples:  $S = \{(\mathbf{x}_i, y_i)\}$ , where  $y_i = \arg\max_c \mathbf{p}_i^{w-cal}$  returns the cluster index producing the largest prediction as the pseudo label for  $\mathbf{x}_i$ .

After selecting high-confidence samples as the pseudo labels, we use the cross-entropy loss to optimize the parameters of the feature extractor and the clustering head:

$$\mathcal{L}_{clu} = -\frac{1}{|S|} \sum_{\mathbf{x}_i \in S} y_i \log \mathbf{p}_i^{s-clu}, \quad (3)$$

where  $|S|$  denotes the total number of selected pseudo-labeled samples,  $\mathbf{p}_i^{s-clu}$  denotes the confidence of the strong augmentation of  $\mathbf{x}_i$  estimated by the clustering head.

### 3.1.2 Calibration Head

In addition to the clustering head, we propose a calibration head with an identical network structure as the clustering head. The calibration head serves the purpose of aligning the output confidence of the model with its true accuracy. However, the well-known calibration methods are not directly applicable here. For example, post-calibration methods like Temperature Scaling require a labeled validation set to tune its hyper-parameter. Meanwhile, the commonly used regularization-based calibration method penalizes the output confidence, rendering the previous pseudo-label selection mechanism invalid.

To this end, we use the K-means algorithm to divide the embeddings matrix (before the clustering head and calibration head) into  $K$  mini-clusters, and record the average output of each mini-cluster in the clustering head as  $\hat{\mathbf{q}}_k = \frac{\sum_{\mathbf{x}_i \in Q_k} \mathbf{p}_i^{clu}}{|Q_k|}$ , where  $Q_k$  denotes the samples belonging to the  $k$ -th mini-cluster and  $|Q_k|$  is the total number of samples in this mini-cluster. Then we take the average prediction of each mini-cluster as the target distribution of the samples in that mini-cluster of the calibration head, i.e.,

$$\mathcal{L}_{cal} = -\frac{1}{B} \sum_k \sum_{\mathbf{x}_i \in Q_k} \hat{\mathbf{q}}_k \log(\mathbf{p}_i^{cal}), \quad (4)$$

where  $\mathbf{p}_i^{cal}$  denotes the output of  $\mathbf{x}_i$  predicted by the calibration head. The above calibration method aligns the feature representation of the samples with their output in the calibration head. Moreover, it will not over-penalize the confidence of the output.

Furthermore, we add a negative entropy loss to make the predicted class distribution more uniform, avoiding all samples being divided into the same cluster:

$$\mathcal{L}_{en} = \frac{1}{C} \sum_{j=1}^C \mathbf{p}_{:,j}^{cal} \log \mathbf{p}_{:,j}^{cal}, \quad (5)$$

where  $\mathbf{p}_{:,j}^{cal}$  denote the  $j$ -th column of the calibration head for a batch of samples. Combining Eqs. (3) and (4), the overall loss of the calibration head is:

$$\mathcal{L} = \mathcal{L}_{cal} + w_{en} \mathcal{L}_{en}, \quad (6)$$

where  $w_{en} \geq 0$  is a hyper-parameter.

**Remark.** It is worth noting that the calibration head differs from the clustering head in its training. While the clustering head selects only high-confident samples for training, the calibration network utilizes all samples during the training process. This is done to obtain a more accurate estimation of the overall confidence and enhance the model’s robustness.

Furthermore, unlike the clustering head, which employs weakly augmented samples to generate pseudo-labels and considers strongly augmented samples as the distribution to be learned, the samples learned by the calibration head undergo no augmentation at all, eliminating any representation differences caused by sample transformations.

### 3.2. Training Process

We first pre-train the backbone network with MoCo-V2, then initialize the clustering and calibration heads using the proposed feature prototype-based initialization strategy, and finally jointly train the dual-head network.

**Feature Prototype-based Initialization.** After pre-training with MoCo-V2, the model is equipped with a feature extractor capable of producing new feature representations to facilitate clustering. However, if we initialize the clustering head and calibration head randomly, they will lack discriminability in clustering from the outset. This becomes particularly problematic as they are responsible for generating pseudo-labels. The random initialization strategy would result in the production of low-quality pseudo-labels and impede the training speed.

To address this issue, we propose to initialize the clustering head and the calibration head with the feature prototype. Specifically, Fig. 3 shows the network structure of the clustering head and the calibration head, which are both a three-layer MLP. For the MLP with  $D$  input units,  $H$  hidden units, and  $C$  output units, we have the intermediate variables  $\mathbf{z} \in \mathbb{R}^{N \times D}$ ,  $\mathbf{h} \in \mathbb{R}^{N \times H}$ ,  $\mathbf{o} \in \mathbb{R}^{N \times C}$ , and two linear layer weights  $\mathbf{W}^{(1)} \in \mathbb{R}^{H \times D}$  and  $\mathbf{W}^{(2)} \in \mathbb{R}^{C \times H}$ . For the first linear layer  $\mathbf{W}^{(1)}$ , we use K-means to find  $H$  prototypes  $\mathbf{r}_\alpha^{(1)} \in \mathbb{R}^D, \alpha = 1, \dots, H$  as the initialization of  $\mathbf{W}^{(1)}$ , i.e.,

$$\mathbf{r}_\alpha^{(1)} = \text{Kmeans}_H(\|\mathbf{z}\|), \quad (7)$$

$$\mathbf{W}_0^{(1)} = \mathbf{0}_{H \times 1}, \mathbf{W}_\alpha^{(1)} = \mathbf{r}_\alpha^{(1)}, \alpha = 1, \dots, H, \quad (8)$$

$$\mathbf{h} = \mathbf{z} \left( \mathbf{W}^{(1)} \right)^\top + \mathbf{W}_0^{(1)}, \quad (9)$$

Note that we set the bias of the linear layer to 0. By the above setting, one neuron of the output will denote a prototype, which means this neuron will indicate the samples within this mini-cluster, and accordingly, this neuron will have the discriminative ability. Besides, the MLP also embeds a BN layer and a ReLU layer, further transforming to get  $\mathbf{h}' = \text{ReLU}(\text{BN}(\mathbf{h}))$ . For the last linear layer of the network, the same operation is also adopted, and finally, the logits output  $\mathbf{o}$  is obtained:

$$\mathbf{r}_\beta^{(2)} = \text{Kmeans}_C(\|\mathbf{h}'\|), \quad (10)$$

$$\mathbf{W}_0^{(2)} = \mathbf{0}_{C \times 1}, \mathbf{W}_\beta^{(2)} = \mathbf{r}_\beta^{(2)}, \beta = 1, \dots, C, \quad (11)$$

$$\mathbf{o} = \mathbf{h}' \left( \mathbf{W}^{(2)} \right)^\top + \mathbf{W}_0^{(2)}. \quad (12)$$

After the initialization with feature prototypes, we further orthogonalize the weights to improve the discriminative ability of the network.

**Joint Optimization.** After the pre-training by MoCo-V2, and the initialization of the clustering head and the calibration head, our model can get preliminary good clustering

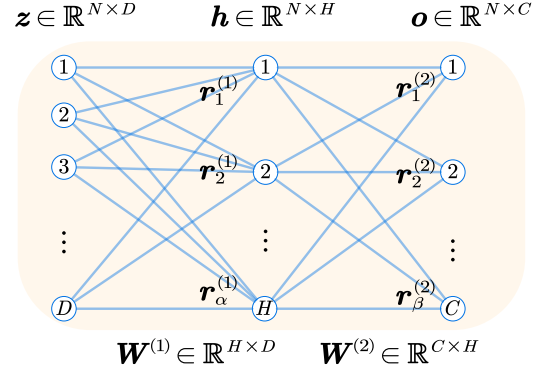


Figure 3. The structure of the clustering head. Note that the calibration head shares the same structure as the clustering head.

results. Then we use the same learning rate to update the parameters of the two MLPs in sequence, using Eq. (3) to optimize the clustering head and feature extractor, and Eq. (6) to optimize the calibration head. The overall training process of our model is summarized in Algorithm 1.

---

#### Algorithm 1: The training of Calibrated Deep Clustering

---

**Data:** Training dataset  $\mathcal{D}_u = \{\mathbf{x}_i : i \in \{1, 2, \dots, N\}\}$

**Input:**  $C$  predefined clusters,  $K$  mini-clusters; Feature extractor  $f(\Theta; \mathbf{x}_i)$ , and classifier  $g(\theta; \cdot)$ .

**Initialization:**

Learning feature extractor  $\Theta$  via representation learning;

Initializing MLPs  $\theta_{clu}$  and  $\theta_{cal}$  with feature prototypes;

**for** epoch  $\leftarrow 1$  **to** EPOCHS **do**

**for**  $b \leftarrow 1$  **to**  $\lfloor N/B \rfloor$  **do**

    Establish batch dataset  $\mathcal{D}_b \subseteq \mathcal{D}_u$ ;

$\mathbf{p}_i^{w-cal} \xleftarrow{\text{no grad.}} \sigma(g(\theta_{cal}; f(\Theta; \mathbf{x}_i^w)))$ ;

    Establish pseudo-labeled samples  $S$  by Eq. (1)-(2);

$\mathbf{z}_i \xleftarrow{\text{no grad.}} f(\Theta; \mathbf{x}_i)$

    Employ K-means on  $\mathbf{z}$  to get partition  $Q_k$ ;

$\mathbf{p}_i^{clu} \xleftarrow{\text{no grad.}} \sigma(g(\theta_{clu}; f(\Theta; \mathbf{x}_i)))$ ;

    Calculate mini-clusters target distribution  $\hat{\mathbf{q}}_k$ ;

**for** sub\_iter  $\leftarrow 1$  **to**  $\lfloor B/B_s \rfloor$  **do**

      Establish sub-batch dataset  $\mathcal{D}_{sub} \subseteq \mathcal{D}_b$ ;

$\mathbf{p}_{sub}^{s-clu} \leftarrow \sigma(g(\theta_{clu}; f(\Theta; \mathbf{x}_{sub}^s)))$ ;

      Calculate  $\mathcal{L}_{clu}$  by Eq. (3), update  $\Theta$  and  $\theta_{clu}$ ;

$\mathbf{p}_{sub}^{cal} \leftarrow \sigma(g(\theta_{cal}; f(\Theta; \mathbf{x}_{sub})))$ ;

      Calculate  $\mathcal{L}_{cal}$  and  $\mathcal{L}_{en}$  by Eqs. (4)-(5), update  $\theta_{cal}$ ;

**end**

**end**

**end**

---

## 4. Experiments

### 4.1. Experiment Settings

**Datasets.** As shown in Tab. 1, we conducted experiments on six widely used benchmark datasets, CIFAR-10 [18],

Table 1. A summary of the datasets

Dataset	Split	#Samples	#Classes	Image Size
CIFAR-10 [18]	Train+Test	60,000	10	32×32
CIFAR-20 [18]	Train+Test	60,000	20	32×32
STL-10 [5]	Train+Test	13,000	10	96×96
ImageNet-10 [2]	Train	13,000	10	224×224
ImageNet-Dogs [2]	Train	19,500	15	224×224
Tiny-ImageNet [6]	Train	100,000	200	64×64

CIFAR-20 [18], STL-10 [5], ImageNet-10 [2], ImageNet-Dogs [2], and Tiny-ImageNet [20]. Similar to [37], we used 20 superclasses of the CIFAR-100 dataset to construct the CIFAR-20, and 10, 15, and 200 subclasses of the ImageNet-1k [6] dataset to extract the ImageNet-10, ImageNet-Dogs, and Tiny-ImageNet. Meanwhile, we extended STL-10 by 100,000 relevant unlabeled data during the pretext training and removed them afterwards. We used the dataset from ImageNet-10, ImageNet-Dogs, and Tiny-ImageNet datasets for both training and testing, while the rest datasets were trained and tested on the merged datasets.

**Backbones.** Similar to [14, 29], we used ResNet-34 and MLP (512d-BN [16]-ReLU [28]-Cd) as the backbone network for all experiments. To facilitate training on small datasets such as CIFAR-10 and CIFAR-20, we modified the first convolution layer’s kernel of the ResNet-34 with with a kernel size of  $3 \times 3$ , padding of 2 and stride of 1, and removed the first max-pooling layer.

**Implementation Details.** The comparison methods can be divided into two types: methods that first learn an embedding by a network and then achieve clustering by using K-means [23]: MoCo-v2 [4], SimSiam [3], BYOL [10] and ProPos [14], and the methods that can achieve clustering and feature learning simultaneously: CC [22], SCAN [37], SeCu [32], and SPICE [29]. For CC, SCAN and SeCu, we re-implemented them with ResNet-34 and MoCo-v2 Pretext to get better results than their original papers for a fair comparison. For SPICE, we used the official trained model since its backbone and pretext are similar to our methods. Furthermore, we trained all the datasets under supervised manner to obtain the upper boundary of cluster performance. More details are shown in the supplementary file.

For CDC, we trained the model for 100 epochs using the Adam optimizer with a learning rate of  $5e-5$  for the encoder,  $1e-4$  for the MLP, and a weight decay of 0. The learning rate of the encoder on CIFAR-20 and Tiny-ImageNet was adjusted to  $1e-5$  for better learning of noisy pseudo labels. Due to the memory limitations of the device, we set  $B = 1,000$  and  $B_s = 500$  for CIFAR-10, CIFAR-20, and STL-10,  $B = 500$  and  $B_s = 125$  for ImageNet-10 and ImageNet-Dogs,  $B = 5,000$  and  $B_s = 1,000$  for Tiny-ImageNet. We set  $K = 500$  for CIFAR-10,  $K = 40$  for

CIFAR-20 and ImageNet-Dogs,  $K = 150$  for STL-10 and ImageNet-10, and  $K = 1,000$  for Tiny-ImageNet. Besides, we set  $M = \lfloor B/C \rfloor$  and  $w_{en} = 1.0$  for all experiments.

**Evaluation Metrics.** We used three common clustering metrics: clustering with clustering Accuracy (ACC) [21], Normalized Mutual Information (NMI) [35], and Adjusted Rand Index (ARI) [15] to evaluate the clustering performance, and used the Expected Calibration Error (ECE) [27] to evaluate the calibration performance. To calculate ECE, all  $N$  samples’ confidence scores are grouped into  $l$  bins and computed by  $ECE = \sum_{i=1}^l \frac{|B_i|}{N} |acc(B_i) - avg.conf.(B_i)|$ , where  $acc(\cdot)$  and  $avg.conf.(\cdot)$  means accuracy and average confidence in each bin.

## 4.2. Main Results

**Clustering Performance.** As shown in Tab. 2, for representation learning methods, significant improvement of clustering performance has already been achieved through K-means. Moreover, the model pre-trained with MoCo-v2 before supervised learning significantly outperforms the plain supervised learning model, all of which demonstrate the importance of representation in deep clustering. For CC and SCAN, we first pre-trained them with MoCo-v2, which achieved a better clustering performance than their original papers. But they are still beaten by the current best deep clustering method SPICE. After applying the same pre-training model, CDC-Cal significantly outperforms CC, SCAN, and SPICE on almost all the datasets. For example, on CIFAR-10 and CIFAR-20 the proposed model outperforms SPICE about 3.4% and 3.3% in ACC and 5.1% and 4.5% in ARI. For larger-scale image datasets, our method also achieves great improvement in clustering performance. For example, compared to SPICE, CDC-Cal has achieved improvements of 1.4%, 11.7%, and 4.8% on ImageNet-10, ImageNet-Dogs, and Tiny-ImageNet. Meanwhile, the results of the clustering head CDC-Clu are close to those of the calibration head CDC-Cal, showing the performance gain of the joint optimization strategy for both heads.

**Calibration Error.** The calibration error of CDC-Cal is far superior to that of CDC-Clu and also superior to that of all the compared methods. CC is not applied the pseudo-labeling strategy, its ECE is relatively low, which to some extent indicates that over-fitting wrong pseudo-labels is a reason for the high ECE. SCAN-3 and SPICE-3 both select high-confidence pseudo-labels for further joint optimization, which does not bring improvement to ECE, especially SPICE-2 uses dual-softmax loss to encourage unambiguous prediction, which leads to more severe overconfidence than SCAN. Our calibration head significantly improves calibration error. For example, compared to SPICE-3 on CIFAR-20, the ECE of our method is about 10 times better. Fig.

Table 2. The clustering performance (ACC, NMI and ARI) and expected calibration error (ECE) on six image benchmarks. The best results are shown in **bold**, while the second best results are underlined.  $\uparrow$  ( $\downarrow$ ) means the higher (resp. lower), the better.

Method	CIFAR-10				CIFAR-20				STL-10				ImageNet-10				ImageNet-Dogs				Tiny-ImageNet			
	ACC $\uparrow$	NMI $\uparrow$	ARI $\uparrow$	ECE $\downarrow$	ACC $\uparrow$	NMI $\uparrow$	ARI $\uparrow$	ECE $\downarrow$	ACC $\uparrow$	NMI $\uparrow$	ARI $\uparrow$	ECE $\downarrow$	ACC $\uparrow$	NMI $\uparrow$	ARI $\uparrow$	ECE $\downarrow$	ACC $\uparrow$	NMI $\uparrow$	ARI $\uparrow$	ECE $\downarrow$	ACC $\uparrow$	NMI $\uparrow$	ARI $\uparrow$	ECE $\downarrow$
MoCo-v2 [4]	82.9	77.7	64.9	N/A	50.7	56.4	26.2	N/A	68.8	69.3	45.5	N/A	56.7	54.1	30.9	N/A	62.8	62.8	48.1	N/A	25.2	43.0	11.0	N/A
Simsiam [3]	70.7	67.7	53.1	N/A	33.0	32.6	16.2	N/A	49.4	61.8	34.9	N/A	78.4	81.7	68.8	N/A	44.2	45.9	27.3	N/A	19.0	36.4	8.4	N/A
BYOL [10]	57.0	65.5	47.6	N/A	34.7	43.9	21.2	N/A	56.3	67.0	38.6	N/A	71.5	70.3	54.1	N/A	58.2	63.4	44.2	N/A	11.2	29.6	4.6	N/A
ProPos [14]	94.3	88.6	88.4	N/A	60.6	<b>61.4</b>	45.1	N/A	86.7	75.8	73.7	N/A	95.6	89.6	90.6	N/A	74.5	69.2	62.7	N/A	29.4	46.0	17.9	N/A
CC [22]	85.2	76.9	72.8	6.2	42.4	47.1	28.4	29.7	80.0	72.7	67.7	11.9	90.6	88.5	85.3	8.1	69.6	65.4	56.0	19.3	12.1	32.5	5.7	<b>3.2</b>
SCAN-2 [37]	84.1	79.3	74.1	10.9	50.0	52.2	34.7	37.1	87.0	78.8	75.6	7.4	95.1	88.9	89.4	2.7	63.3	60.1	49.6	26.4	27.6	43.1	15.3	27.4
SeCu-Size [32]	90.0	83.2	81.5	8.1	52.9	54.9	38.4	<u>13.1</u>	-	-	-	-	-	-	-	-	-	-	-	-	-	-	-	-
SPICE-2 [29]	84.4	73.5	70.9	15.4	47.6	44.3	30.3	52.3	89.6	80.4	79.2	10.1	92.1	82.8	83.6	7.8	64.6	56.9	47.7	35.3	30.5	44.9	16.3	48.5
SCAN-3 [37]	90.3	82.5	80.8	6.7	51.2	51.2	35.6	39.0	91.4	83.6	82.5	6.6	97.0	92.5	93.6	<u>1.5</u>	72.2	67.4	58.7	19.5	25.8	40.7	13.4	48.8
SeCu [32]	92.6	86.2	85.4	4.9	52.7	56.7	39.7	41.8	-	-	-	-	-	-	-	-	-	-	-	-	-	-	-	-
SPICE-3 [29] <sup>1</sup>	91.5	85.4	83.4	7.8	58.4	57.6	42.2	40.6	<u>93.0</u>	<b>86.1</b>	85.5	6.3	95.9	90.2	91.2	4.1	67.5	62.6	52.6	32.5	29.1	42.7	14.7	N/A
CDC-Clu (Ours)	94.9	89.3	89.4	1.4	<b>61.9</b>	60.6	<b>46.7</b>	28.0	<b>93.1</b>	86.0	<b>85.8</b>	4.8	<u>97.2</u>	93.1	94.0	1.8	<b>79.3</b>	<b>76.7</b>	<b>70.3</b>	<u>17.1</u>	<b>34.0</b>	<u>47.2</u>	<b>20.0</b>	37.8
CDC-Cal (Ours)	<b>94.9</b>	<b>89.3</b>	<b>89.5</b>	<b>1.1</b>	61.7	60.9	46.6	<b>4.9</b>	93.0	85.8	85.6	<b>0.9</b>	<b>97.3</b>	<b>93.2</b>	<b>94.1</b>	<b>0.8</b>	79.2	76.5	70.0	<b>7.7</b>	33.9	<b>47.5</b>	19.9	11.0
Supervised	89.8	79.1	79.2	1.8	73.7	62.6	53.6	7.4	80.4	67.3	62.2	10.0	99.2	97.7	98.3	0.9	93.1	86.6	85.7	0.9	47.7	59.3	24.3	5.2
+MoCo-v2	94.5	87.8	88.3	1.7	84.4	74.8	70.5	4.9	90.5	81.7	80.6	3.5	99.9	99.7	99.8	0.4	99.5	98.7	99.0	0.9	53.8	64.0	30.9	8.4

<sup>1</sup> SPICE-3 (Joint training) used WideResNet-28-2 for Cifar10, WRN-28-8 for CIFAR-20, and WRN-37-2 for STL-10.

Table 3. The ablation results of Initialization.

Initialization Strategy	CIFAR-10		CIFAR-20		STL-10	
	ACC $\uparrow$	ECE $\downarrow$	ACC $\uparrow$	ECE $\downarrow$	ACC $\uparrow$	ECE $\downarrow$
w/o Init.	19.1	8.5	10.4	4.9	19.2	8.5
CDC-Clu (w/o Init.)	89.4	7.0	44.0	44.8	73.5	22.6
CDC-Cal (w/o Init.)	89.4	3.3	44.4	11.9	73.3	17.9
CDC-Only K-means	85.8	33.8	54.1	30.8	88.9	29.6
CDC-Init	87.2	63.7	56.4	45.6	89.8	62.8
CDC-Clu (with Init.)	94.9	1.4	61.9	28.0	93.1	4.8
CDC-Cal (with Init.)	94.9	1.1	61.7	4.9	93.0	0.9

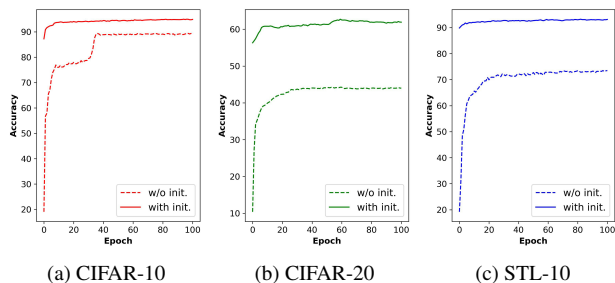


Figure 4. The training process with Init. and w/o Init.

1 provides a visual comparison of the ECE on CIFAR-20, where we can find our method not only achieves superior reliability but also better clustering performance.

### 4.3. Ablation Study

**Effect of Initialization.** As shown in Tab. 3, simply performing K-means on the learned features to initialize the weights can bring about a significant improvement in clustering performance. The accuracy can be further improved with the aid of orthogonalization techniques for weights (CDC-Init). Moreover, training for 100 epochs under the same settings, the model without initialization performs worse (shown in Fig. 4) and sometimes inferior

to CDC-Init, which shows the initialization strategy is not only efficient but also robust to local optima.

**Single Network is trade-off on clustering performance and calibration error.** We focus on the pseudo-labeling process of the SCAN model and train with a rejection threshold of 0.99, evaluating the clustering performance and calibration error of the single network model after applying calibration loss. The results are shown in Tab. 4. Different calibration losses show a similar trend: the larger the calibration parameter, the greater the penalty for the sample confidence. However, this does not guarantee a reduction in calibration error, because the overall decrease in sample confidence level will reduce the number of samples above the threshold, and the lack of sample sampling rate seriously harms the performance of the model. For example, after applying LS on CIFAR-20, the model degrades to a trivial solution. This indicates that a single loss is difficult to optimize the two objectives of clustering and calibration at the same time. Therefore, our method uses a dual-head to decouple them and continuously improve clustering performance and calibration error.

**Effect of Confidence-aware Selection.** Tab. 5 demonstrates that fixed thresholds are limited by the difficulty of the dataset being learned. More challenging datasets require higher thresholds to filter out noisy labels, while easier datasets need lower thresholds to obtain sample diversity. Our method measures the average confidence of a group of samples with the highest confidence, which can increase the sample utilization rate of each class under accurate confidence estimation.

**Effect of Calibration Head Loss.** We evaluated the effectiveness of regularization methods by merely changing the calibration loss of the calibration head, as shown in the bottom row of Tab. 5. Although these methods can reduce calibration errors, their performance does not significantly improve. This is related to the penalty imposed on high-

Table 4. The results obtained after adding calibration loss with a threshold of 0.99 to the SCAN, (-) denotes the calibration parameters we used, "CONF" denotes the average maximum softmax probability of the test samples.

Module	Settings	CIFAR-10					CIFAR-20					STL-10				
		ACC ↑	NMI ↑	ARI ↑	ECE ↓	CONF	ACC ↑	NMI ↑	ARI ↑	ECE ↓	CONF	ACC ↑	NMI ↑	ARI ↑	ECE ↓	CONF
Single Network	Initial	84.08	79.34	74.10	10.92	94.99	49.99	52.19	34.67	37.11	87.10	86.96	78.81	75.63	7.40	94.36
	CE (Thre. = 0.99)	89.38	80.86	79.04	6.79	96.16	50.50	50.00	34.45	38.07	88.57	90.49	82.26	80.74	6.16	96.65
	Label Smoothing (0.006)	89.25	79.76	78.61	5.42	94.67	46.33	45.46	29.77	35.00	81.33	89.92	81.14	79.88	5.31	95.23
	Label Smoothing (0.007)	87.70	77.90	75.66	6.64	94.34	12.98	8.62	2.63	5.91	7.08	88.98	79.84	78.26	5.80	94.78
	Label Smoothing (0.008)	87.17	76.70	74.68	6.80	93.96	8.35	2.76	0.60	2.63	5.92	88.79	79.65	77.62	5.33	94.11
	CE+L1 Norm (0.005)	88.43	77.56	76.74	3.70	91.61	45.90	42.19	28.05	27.74	73.64	77.12	68.44	61.57	13.46	90.46
	CE+L1 Norm (0.006)	86.43	74.57	72.94	4.52	89.58	41.97	38.65	24.45	29.48	70.78	79.29	71.29	66.16	9.45	88.38
CE+L1 Norm (0.007)	85.63	73.40	71.24	4.96	86.82	41.70	41.42	27.50	28.68	69.45	70.02	63.99	55.06	13.48	81.53	

Table 5. The ablation results of sample selection strategy and calibration head loss after the same initialization (CDC-Init).

Module	Settings	CIFAR-10				CIFAR-20				STL-10			
		ACC ↑	NMI ↑	ARI ↑	ECE ↓	ACC ↑	NMI ↑	ARI ↑	ECE ↓	ACC ↑	NMI ↑	ARI ↑	ECE ↓
Dual-head Network	Fixed Thre. (0.99)	80.6	69.8	65.8	6.5	54.9	55.9	37.1	15.1	89.6	81.0	79.3	1.0
	Fixed Thre. (0.95)	91.9	85.2	83.9	3.5	50.8	49.2	30.5	12.6	91.8	84.0	83.3	1.1
	Fixed Thre. (0.90)	92.7	86.5	85.3	3.2	43.3	43.2	27.3	4.1	93.0	86.1	85.7	1.0
	Fixed Thre. (0.80)	93.6	87.5	86.9	1.7	49.9	50.5	33.6	3.9	93.0	86.1	85.7	2.0
	CDC-Cal (Ours)	94.9	89.3	89.5	1.1	61.7	60.9	46.6	4.9	93.0	85.8	85.6	0.9
	CDC-Label Smoothing	84.3	77.3	72.1	3.1	56.6	58.2	40.7	5.4	92.5	85.1	84.5	0.7
	CDC-Focal Loss	82.5	76.8	70.5	2.8	54.4	56.0	38.8	2.7	92.0	84.4	83.6	1.2
	CDC-L1 Norm	87.4	79.9	76.2	2.6	58.2	59.5	42.7	11.5	93.0	85.8	85.4	0.8

confidence samples by these methods: over-penalizing high-confidence samples, which is evident in the reliability diagram in Fig. 5. Since samples with similar features are more likely to have consistent outputs, our method imposes a smaller penalty on high-confidence samples than on low-confidence samples, which effectively maintains the output of reliable samples.

## 5. Conclusion

In this paper, we have introduced a novel calibrated deep clustering model that outperforms SOTA deep clustering models in terms of clustering performance. Notably, our model is the first deep clustering method capable of calibrating the output confidence. In particular, our model demonstrates an expected calibration error that is 10 times better than certain compared methods. To achieve these results, we proposed a dual-head clustering network consisting of a clustering head and a calibration head. The clustering head utilizes the calibrated confidence estimated by the calibration head to select highly reliable pseudo-labels. The calibration head, on the other hand, calibrates the output confidence of all samples using a novel regularization loss. Additionally, we introduced an effective initialization strategy for both the clustering head and the calibration head, significantly accelerating the overall training speed. Through our calibrated deep clustering neural network, the output confidence of the model is well aligned with its true accuracy, which means we can trustfully judge when we can

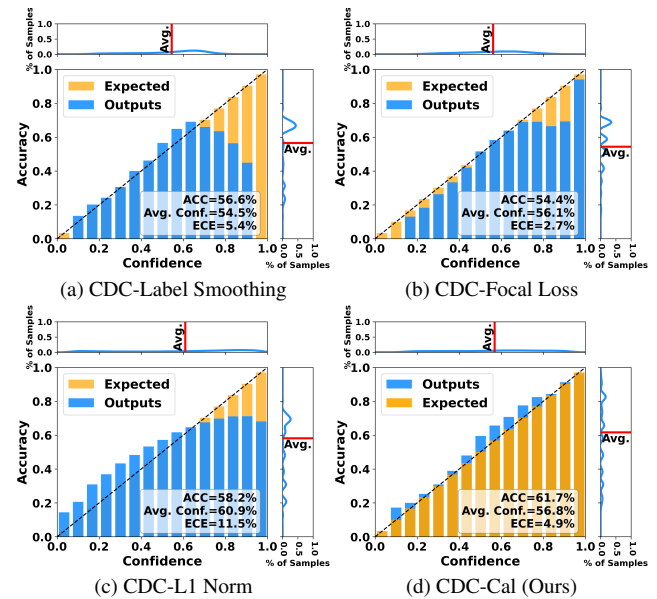


Figure 5. Reliability diagrams on CIFAR-20 with the calibration head applied different regularization losses. In the high-confidence region, all compared calibration losses face a decline in clustering accuracy.

rely on the prediction of the model. Moreover, as we do not need any label to train the network, the above benefit can be gained quite easily.

## References

- [1] Nabil Alami, Mohammed Meknassi, Noureddine Ennahnahi, Yassine El Adlouni, and Ouafae Ammor. Unsupervised neural networks for automatic arabic text summarization using document clustering and topic modeling. *Expert Systems with Applications*, 172:114652, 2021. [2](#)
- [2] Jianlong Chang, Lingfeng Wang, Gaofeng Meng, Shiming Xiang, and Chunhong Pan. Deep adaptive image clustering. In *ICCV*, pages 5880–5888, 2017. [6](#)
- [3] Ting Chen, Simon Kornblith, Mohammad Norouzi, and Geoffrey Hinton. A simple framework for contrastive learning of visual representations. In *ICML*, pages 1597–1607, 2020. [6, 7](#)
- [4] Xinlei Chen, Haoqi Fan, Ross Girshick, and Kaiming He. Improved baselines with momentum contrastive learning. *arXiv preprint arXiv:2003.04297*, 2020. [3, 6, 7](#)
- [5] Adam Coates, Andrew Ng, and Honglak Lee. An analysis of single-layer networks in unsupervised feature learning. In *International Conference on Artificial Intelligence and Statistics*, pages 215–223, 2011. [6](#)
- [6] Jia Deng, Wei Dong, Richard Socher, Li-Jia Li, Kai Li, and Li Fei-Fei. Imagenet: A large-scale hierarchical image database. In *CVPR*, pages 248–255, 2009. [6](#)
- [7] Zhipeng Ding, Xu Han, Peirong Liu, and Marc Niethammer. Local temperature scaling for probability calibration. In *ICCV*, pages 6889–6899, 2021. [2](#)
- [8] Di Feng, Lars Rosenbaum, Claudius Glaeser, Fabian Timm, and Klaus Dietmayer. Can we trust you? on calibration of a probabilistic object detector for autonomous driving. *arXiv preprint arXiv:1909.12358*, 2019. [2](#)
- [9] Jakob Gawlikowski, Cedric Rovile Njjeutcheu Tassi, Mohsin Ali, Jongseok Lee, Matthias Humt, Jianxiang Feng, Anna Kruspe, Rudolph Triebel, Peter Jung, Ribana Roscher, et al. A survey of uncertainty in deep neural networks. *arXiv preprint arXiv:2107.03342*, 2021. [2](#)
- [10] Jean-Bastien Grill, Florian Strub, Florent Althé, Corentin Tallec, Pierre Richemond, Elena Buchatskaya, Carl Doersch, Bernardo Avila Pires, Zhaohan Guo, Mohammad Gheshlaghi Azar, et al. Bootstrap your own latent—a new approach to self-supervised learning. *NeurIPS*, 33:21271–21284, 2020. [6, 7](#)
- [11] Chuan Guo, Geoff Pleiss, Yu Sun, and Kilian Q Weinberger. On calibration of modern neural networks. In *ICML*, pages 1321–1330, 2017. [2](#)
- [12] Xifeng Guo, Long Gao, Xinwang Liu, and Jianping Yin. Improved deep embedded clustering with local structure preservation. In *IJCAI*, pages 1753–1759, 2017. [2](#)
- [13] Peihao Huang, Yan Huang, Wei Wang, and Liang Wang. Deep embedding network for clustering. In *2014 International Conference on Pattern Recognition*, pages 1532–1537, 2014. [2](#)
- [14] Zhizhong Huang, Jie Chen, Junping Zhang, and Hongming Shan. Learning representation for clustering via prototype scattering and positive sampling. *IEEE Transactions on Pattern Analysis and Machine Intelligence*, 2022. [1, 6, 7](#)
- [15] Lawrence Hubert and Phipps Arabie. Comparing partitions. *Journal of classification*, 2:193–218, 1985. [6](#)
- [16] Sergey Ioffe and Christian Szegedy. Batch normalization: Accelerating deep network training by reducing internal covariate shift. In *ICML*, pages 448–456, 2015. [6](#)
- [17] Taejong Joo and Uijung Chung. Revisiting explicit regularization in neural networks for well-calibrated predictive uncertainty. *arXiv preprint arXiv:2006.06399*, 2020. [3](#)
- [18] Alex Krizhevsky, Geoffrey Hinton, et al. Learning multiple layers of features from tiny images. 2009. [5, 6](#)
- [19] Ananya Kumar, Percy S Liang, and Tengyu Ma. Verified uncertainty calibration. *NeurIPS*, 32, 2019. [2](#)
- [20] Ya Le and Xuan Yang. Tiny imagenet visual recognition challenge. *CS 231N*, 7(7):3, 2015. [6](#)
- [21] Tao Li and Chris Ding. The relationships among various nonnegative matrix factorization methods for clustering. In *ICDM*, pages 362–371, 2006. [6](#)
- [22] Yunfan Li, Peng Hu, Zitao Liu, Dezhong Peng, Joey Tianyi Zhou, and Xi Peng. Contrastive clustering. In *AAAI*, pages 8547–8555, 2021. [1, 2, 6, 7](#)
- [23] Stuart Lloyd. Least squares quantization in pcm. *IEEE Transactions on Information Theory*, 28(2):129–137, 1982. [6](#)
- [24] Takahiro Mimori, Keiko Sasada, Hirotaka Matsui, and Issei Sato. Diagnostic uncertainty calibration: Towards reliable machine predictions in medical domain. In *International Conference on Artificial Intelligence and Statistics*, pages 3664–3672, 2021. [2](#)
- [25] Jishnu Mukhoti, Viveka Kulharia, Amartya Sanyal, Stuart Golodetz, Philip Torr, and Puneet Dokania. Calibrating deep neural networks using focal loss. *NeurIPS*, 33:15288–15299, 2020. [2](#)
- [26] Rafael Müller, Simon Kornblith, and Geoffrey E Hinton. When does label smoothing help? *NeurIPS*, 32, 2019. [2](#)
- [27] Mahdi Pakdaman Naeini, Gregory Cooper, and Milos Hauskrecht. Obtaining well calibrated probabilities using bayesian binning. In *AAAI*, 2015. [6](#)
- [28] Vinod Nair and Geoffrey E Hinton. Rectified linear units improve restricted boltzmann machines. In *ICML*, pages 807–814, 2010. [6](#)
- [29] Chuang Niu, Hongming Shan, and Ge Wang. Spice: Semantic pseudo-labeling for image clustering. *IEEE Transactions on Image Processing*, 31:7264–7278, 2022. [1, 2, 3, 6, 7](#)
- [30] Bo Peng, Jianjun Lei, Huazhu Fu, Yalong Jia, Zongqian Zhang, and Yi Li. Deep video action clustering via spatio-temporal feature learning. *Neurocomputing*, 456:519–527, 2021. [2](#)
- [31] Gabriel Pereyra, George Tucker, Jan Chorowski, Łukasz Kaiser, and Geoffrey Hinton. Regularizing neural networks by penalizing confident output distributions. *arXiv preprint arXiv:1701.06548*, 2017. [2](#)
- [32] Qi Qian. Stable cluster discrimination for deep clustering. In *CVPR*, 2023. [1, 2, 3, 6, 7](#)
- [33] Seonguk Seo, Paul Hongsuck Seo, and Bohyung Han. Learning for single-shot confidence calibration in deep neural networks through stochastic inferences. In *CVPR*, pages 9030–9038, 2019. [2](#)
- [34] Yuming Shen, Ziyi Shen, Menghan Wang, Jie Qin, Philip Torr, and Ling Shao. You never cluster alone. *NeurIPS*, 34:27734–27746, 2021. [2](#)

- [35] Alexander Strehl and Joydeep Ghosh. Cluster ensembles—a knowledge reuse framework for combining multiple partitions. *Journal of machine learning research*, 3(Dec):583–617, 2002. [6](#)
- [36] Fei Tian, Bin Gao, Qing Cui, Enhong Chen, and Tie-Yan Liu. Learning deep representations for graph clustering. In *AAAI*, 2014. [2](#)
- [37] Wouter Van Gansbeke, Simon Vandenhende, Stamatios Georgoulis, Marc Proesmans, and Luc Van Gool. Scan: Learning to classify images without labels. In *ECCV*, pages 268–285, 2020. [1](#), [2](#), [3](#), [6](#), [7](#)
- [38] Junyuan Xie, Ross Girshick, and Ali Farhadi. Unsupervised deep embedding for clustering analysis. In *ICML*, pages 478–487, 2016. [1](#), [2](#)
- [39] Shengjia Zhao, Tengyu Ma, and Stefano Ermon. Individual calibration with randomized forecasting. In *ICML*, pages 11387–11397, 2020. [2](#)